Physica E 42 (2010) 719–721

Contents lists available at ScienceDirect

Physica E

journal homepage: www.elsevier.com/locate/physe

Negative terahertz dynamic conductivity in electrically induced lateral p–i–n junction in graphene

Victor Ryzhii [a,*], Maxim Ryzhii [a], Michael S. Shur [b], Vladimir Mitin [c]

[a] Computational Nanoelectronics Laboratory, University of Aizu, Aizu-Wakamatsu 965-8580, and Japan Science and Technology Agency, CREST, Tokyo 107-0075, Japan
[b] Department of Electrical, Electronics, and Systems Engineering, Rensselaer Polytechnic Institute, Troy 12180, USA
[c] Department of Electrical Engineering, University at Buffalo, Buffalo 14260, USA

ARTICLE INFO

Available online 18 November 2009

Keywords:
Graphene
Tunneling
Transit-time device
Dynamic conductivity
Plasma oscillations
Terahertz radiation

ABSTRACT

We analyze a graphene tunneling transit-time device based on a heterostructure with a lateral p–i–n junction electrically induced in the graphene layer and calculate its ac characteristics. Using the developed device model, it is shown that the ballistic transit of electrons and holes generated due to interband tunneling in the i-section results in the negative ac conductance in the terahertz frequency range. The device can serve as an active element of terahertz oscillators

1. Introduction

Theoretical predictions and experimental observations of unique properties of graphene-based structures, in particular, the possibility of ballistic electron and hole transport in fairly large samples at room temperatures (see, for instance, Refs. [1–3]) stimulate proposals of novel graphene electron and optoelectron devices. In this paper, we consider a tunneling transit-time device based on a gated graphene with electrically induced lateral p–i–n junction and present the device dynamic characteristics, the frequency dependences of the real and imaginary parts of the ac conductance, calculated using the developed device model. In the graphene tunneling transit-time (G-TUNNETT) device under consideration, the depleted i-section of the graphene layer play the role of both the tunneling injector and the transit region at the same time.

Extending the device model used by us recently [4] (mainly by the inclusion into the consideration of the nonuniformity of the electric field in the i-section and the possibility of the self-excitation of plasma oscillations in the gated p- and n-sections), we show that the G-TUNNETT can exhibit negative ac conductance in the terahertz (THz) range of frequencies and, hence, serve as an active element in THz oscillators.

* Corresponding author.
E-mail address: v-ryzhii@u-aizu.ac.jp (V. Ryzhii).

1386-9477/$ - see front matter © 2009 Elsevier B.V. All rights reserved.
doi:10.1016/j.physe.2009.11.032

2. Device model and terminal ac conductance

The G-TUNNETT structure under consideration is shown schematically in Fig. 1(a). It is assumed that the gate–source voltage ($V_p<0$) and the drain–gate voltage ($V_n>0$) are applied. This results in creating the hole and electron two-dimensional systems (with the Fermi energy ε_F), i.e., the p- and n-regions in the channel sections under the pertinent gates. Under the reverse source–drain voltage ($V>0$), a lateral p–i–n junction is formed, which corresponds to the band diagram shown in Fig. 1(b). It is assumed that apart from a dc component $V_0>0$ which corresponds to a reverse bias, the net source–drain voltage V comprises also an ac component $\delta V \exp(-i\omega t)$: $V=V_0+\delta V_\omega \exp(-i\omega t)$, where δV_ω and ω are the signal amplitude and frequency, respectively.

The probability of interband tunneling in graphene is a fairly sharp function of the angle between the direction of the electron (hole) motion and the x-direction (from the source to the drain) [5]. Taking this into account, we disregard some spread in the x-component of the velocity of the injected electrons and assume that all the generated electrons and holes propagate in the x-direction with the velocity $v_x \simeq v_W$, where $v_W \simeq 10^8$ cm/s is the characteristic velocity of the electron and hole spectra in graphene. Considering the formula for the interband tunneling probability [5], we assume that the rate of the local tunneling generation of electron hole pairs $G/2l \propto \mathcal{E}^{3/2}$, where $2l$ is the length of the depleted i-section and $\mathcal{E}$ is the electric field in the i-section. In the structures with the spacing between the top gates $D \gg W_t, l_s$, where W_t is the thickness of the layers separating the graphene layer and the gates and l_s is the characteristic screening

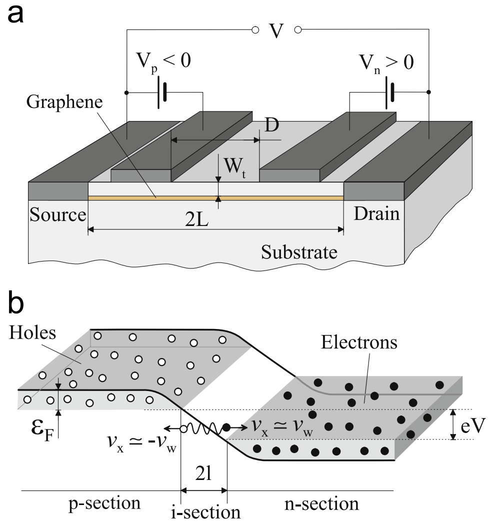

Fig. 1. Structure of a G-TUNNETT device (a) and its band diagram under the reverse bias (b). Arrows with wavy tail indicate the directions of propagation of the generated electrons and holes generated due to interband tunneling.

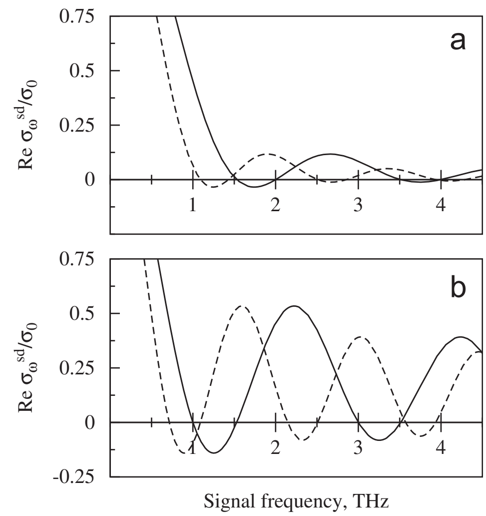

Fig. 2. Real part of the ac conductance σ_ω^{sd} versus the signal frequency $f=\omega/2\pi$ calculated for uniform (a) and strongly nonuniform (b) electric-field spatial distributions in the i-section for different lengths of i-section: solid lines correspond to $2l=0.5\,\mu$m ($\tau=0.25$ ps) and dashed lines correspond to $2l=0.7\,\mu$m ($\tau=0.35$ ps).

lengths, one can assume $2l \simeq D$ (as for the problem of screening in two-dimensional electron and hole systems, see, for instance, Refs. [6,7]). One can expect that this is valid when the dc conductivity of the p- and n-sections is much higher than the dc conductivity of the intrinsic graphene. Actually, the length of the depleted high-electric field i-section $2l$ depends also on V_0. However, we disregard this effect. In the case of ballistic electron and hole transport in the i-section when the generated electrons and holes do not change the directions of their propagation, the continuity equations governing the ac components of the electrons and holes densities $\delta\Sigma_\omega^-$ and $\delta\Sigma_\omega^+$ can be presented as

$$-i\omega\delta\Sigma_\omega^\mp \pm v_W\frac{d\delta\Sigma_\omega^\mp}{dx} = \frac{3G_0}{4l}\frac{\delta V_\omega}{V_0}. \tag{1}$$

Here $G_0=G_0(x)$ and δG_ω are the dc and ac components of the local tunneling rate, respectively. The boundary conditions are as follows: $\delta\Sigma_\omega^\mp|_{x=\mp l}=0$.

We shall consider Eq. (1) in the following two limiting cases: (a) the nonuniformity of the electric field in the i-section is insignificant, so that the components of the latter can be estimated as $\mathcal{E}_0 \simeq V_0/2l$ and $\delta\mathcal{E}_\omega \simeq \delta V_\omega/2l$, and (b) the electric field exhibits strong maxima near the edges of the n- and p-sections. In the former case, the tunneling generation of electrons and holes takes place in the whole i-section, whereas in the latter case, the electrons and holes are primarily generated at the points $|x| \lesssim l$.

Solving Eq. (2) in the case "a" and using the Shockley-Ramo theorem for the induced current, the real and imaginary parts of the ac (dynamic) component of the source–drain (terminal) conductance $\sigma_\omega^{sd}=\delta J_\omega^{sd}/\delta V_\omega$ can be presented as

$$\mathrm{Re}\,\sigma_\omega^{sd} = \frac{3\sigma_0}{2}\frac{\sin(\omega\tau)}{\omega\tau}\mathcal{J}_0(\omega\tau), \tag{2}$$

$$\mathrm{Im}\,\sigma_\omega^{sd} = \frac{3\sigma_0}{2}\left[\frac{1\text{-}\cos(\omega\tau)\mathcal{J}_0(\omega\tau)}{\omega\tau}\text{-}c\omega\tau\right]. \tag{3}$$

Here $\sigma_0=J_0/V_0$ is the dc conductance, J_0 is the dc current, $c=2C/3\sigma_0\tau$, C is the lateral p–i–n junction capacitance, $\mathcal{J}_0(\xi)$ is the Bessel function, and $\tau=l/v_W$ is the characteristic transit time of electrons and holes across the i-section. In the case "b", instead of Eq. (3), we arrive at

$$\mathrm{Re}\,\sigma_\omega^{sd} = \frac{3\sigma_0}{2}\cos(\omega\tau)\mathcal{J}_0(\omega\tau), \tag{4}$$

$$\mathrm{Im}\,\sigma_\omega^{sd} = \frac{3\sigma_0}{2}[\sin(\omega\tau)\mathcal{J}_0(\omega\tau)\text{-}c\omega\tau]. \tag{5}$$

Fig. 2 shows the real part of the ac conductance σ_ω^{sd} (normalized by its ac value) as a function of the signal frequency $f=\omega/2\pi$ calculated for G-TUNNETTs with $2l=0.5$ and $0.7\,\mu$m (this corresponds to $\tau=0.25$ and 0.35 ps, respectively) and using Eqs. (3) and (5). As seen, the real part of the ac conductance exhibits a pronounced oscillatory behavior with the frequency ranges where it has different signs. The real part of the ac conductance can be negative in the THz range of frequencies in the G-TUNNETT structures with the i-section length only moderately smaller than $1\,\mu$m. As follows from Eq. (3) and Fig. 2 in the case "a", the relative value of the real part of the ac conductance, corresponding to the first minima, for $l=0.25\,\mu$m is $\mathrm{Re}\,\sigma_{\omega=2\pi f_1}^{sd}/\sigma_0 \simeq$ -0.034 at the frequency $\omega/2\pi=f_1\simeq 1.75$ THz and $\mathrm{Re}\,\sigma_{\omega=2\pi f_1}^{sd}/\sigma_0 \simeq$ -0.141 at the frequency $\omega/2\pi=f_1\simeq 1.25$ THz in the case "b", respectively. At $V_0=0.2$ V, one can obtain $\sigma_0 \simeq 3\times10^{12}\,\mathrm{s}^{-1}$ and $\mathrm{Re}\,\sigma_{\omega=2\pi f_1}^{sd} \simeq -1\times10^{11}\,\mathrm{s}^{-1}$. In the case "b", Eq. (5) (see also Fig. 2) for the same parameters and the same dc current yields $f_1 \simeq 1.25$ THz, $\mathrm{Re}\,\sigma_{\omega=2\pi f_1}^{sd}/\sigma_0 \simeq$ -0.141, and $\mathrm{Re}\,\sigma_{\omega=2\pi f_1}^{sd} \simeq -4\times 10^{11}\,\mathrm{s}^{-1}$. A significant difference in the absolute values of $\mathrm{Re}\,\sigma_{\omega=2\pi f_1}^{sd}/\sigma_0$ in the limiting cases under consideration is associated with the following. In the case "a", there is a marked spread Δt_{tr} in the transit times of electrons and holes generated at different points of the i-section: $\Delta t_{tr}^{(a)} \simeq \tau$. However, in the case "b", $\Delta t_{tr}^{(b)} \ll \tau$, so that the oscillations of $\mathrm{Re}\,\sigma_\omega$ are more pronounced. Smaller value of f_1 in the case "b" is due a longer average transit time: $t_{tr}^{(b)} \simeq 2\tau$, while $t_{tr}^{(a)} \simeq \tau$.

3. Self-excitation of plasma oscillations

The fundamental plasma frequency in the gated p- and n-sections, in which the spectrum of the plasma waves is a sound-like with the characteristic velocity s and the characteristic plasma frequency $\Omega=\pi s/2(L\text{-}l)$. At sufficiently high gate voltages when the electron (hole) Fermi energy in the n-section (p-section) $\varepsilon_F = (\hbar v_W/2\sqrt{2})\sqrt{æV_t/eW_t} \gg k_BT$, one obtains $s \simeq \sqrt{2e^2W_t\varepsilon_F/æ\hbar^2}$

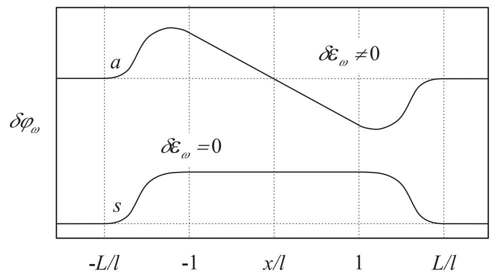

Fig. 3. Qualitative view of spatial distributions of the ac potential for asymmetrical and symmetrical modes.

$> v_W$ [8], where $2L$ is the spacing between the source and drain contacts, T is the temperature, and k_B is the Boltzmann constant. Since the plasma frequency in graphene can be rather large (owing to a large s), the condition $\omega < \Omega$ assumed above can be easily fulfilled for the signal frequencies in the THz range (as well as the condition $\omega \simeq \Omega$) by a proper choice of the device structure length $2L$ and the gate voltage V_t. Indeed, setting, for example, $s = 8 \times 10^8$ cm/s, and $L\text{-}l = 1\,\mu$m, one can obtain $\Omega/2\pi = 4$ THz.

If the frequencies $f_1, f_2, \ldots$, which correspond to the pertinent minimum in the $\mathrm{Re}\,\sigma_\omega$ versus ω dependence, are far from the resonant plasma frequency $\Omega/2\pi$, the quasi-neutral p- and n-sections serve as the highly conducting contacts. However, when $f_1 \sim \Omega/2\pi$ (or $f_2 \sim \Omega/2\pi$), i.e., when the frequency of the plasma oscillations falls into the range where $\mathrm{Re}\,\sigma_\omega^{sd} < 0$, the hole and electron systems in the gated p- and n-sections, respectively, can play the role of the plasma resonators [9]. In this situation, the self-excitation of the plasma oscillations (plasma instability) can be possible [10]. Indeed, taking into account that the Drude conductance of the gated p- and n-sections is equal to $\sigma_\omega^D = \sigma_0^D[i/(\omega + i\nu)\tau]$, where $\sigma_0^D = (e^2 p_F/\pi\hbar^2)[l/(L\text{-}l)]$ is the characteristic Drude dc conductance of the gated graphene section with the Fermi momentum p_F and ν is the frequency of hole and electron collisions with defects and acoustic phonons, one can arrive at the following dispersion equation for the plasma oscillations in the gated p- and n-sections with the frequency ω:

$$\sqrt{\frac{\omega}{\omega + i\nu}}\cot\left[\frac{\pi\sqrt{\omega(\omega + i\nu)}}{2\Omega}\right] = i\mathcal{R}\mathcal{F}(\omega\tau), \tag{6}$$

where $\mathcal{R} = \sigma_0/\sigma_0^D = (6\hbar^2\sigma_0/e^2 p_F)[(L\text{-}l)/l]$, $\mathcal{F}(\omega\tau) = \sin(\omega\tau)\mathcal{J}_0(\omega\tau)$, and $\mathcal{F}(\omega\tau) = (\omega\tau)\cos(\omega\tau)\mathcal{J}_0(\omega\tau)$ in the cases "a" and "b", respectively. Using the expression for the dc tunneling current [4], $\mathcal{R}$ can be expressed via the dc source–drain voltage V_0 and the electron and hole density in the gated sections Σ_0 as $\mathcal{R} = (3/2^{3/2}\pi^3)\sqrt{(eV_0/v_W l\Sigma_0\hbar)}[(L\text{-}l)/l]$ (since it is assumed that the dc voltage drops primarily across the depleted i-section, the $R \ll 1$). Assuming that $\Sigma_0 = 5 \times 10^{11}\,\mathrm{cm}^{-2}$, $l = 0.25\,\mu$m, $L\text{-}l = 2.35\,\mu$m, (for $s = 6 \times 10^8$ cm/s, this corresponds to $f = 1.25$ THz) and $V_0 = 0.2\text{-}0.8$ V, one obtains $R \simeq 0.16\text{-}0.32$. Here we have neglected the contribution of electrons and holes in the i-section to its capacitance as well as the geometrical capacitance of this section, which are small in comparison with the gated p- and n-sections capacitance. When $\Omega \gg \nu$ (i.e., $Q = 4\Omega/\pi\nu \gg 1$), Eq. (7) yields $\mathrm{Re}\,\omega \simeq (2n\text{-}1)\Omega$, where $n = 1, 2, 3, \ldots$ is the plasma mode index. Simultaneously, from Eq. (6) we obtain the following expressions for the damping/growth rate $\gamma = \mathrm{Im}\,\omega$ of plasma oscillations (with $n = 1$): $\gamma = \text{-}\nu/2\text{-}\mathcal{R}\,\Omega\,\mathcal{F}(\Omega\tau)\pi$ for the oscillations with the asymmetrical distribution of the ac potential $\delta\varphi_\omega$ corresponding to the upper curve in Fig. 3 with the in-plane ac electric field in the i-section ($\text{-}l < x < l$) $\delta\mathcal{E}_\omega \neq 0$ (the phases of oscillation in the p- and n-sections are opposite), and $\gamma \simeq \text{-}\nu/2$ for the oscillations (damped) with the symmetrical distributions of the ac potential (see the lower curve in Fig. 3) and $\delta\mathcal{E}_\omega = 0$. Using this, we arrive at the following condition of the plasma oscillations self-excitation: $Q > 2[\mathcal{R}|\min\mathcal{F}(\Omega\tau)|]^{-1}$. As follows from the latter inequality, the self-excitation of plasma oscillations (plasma instability) can occur if their quality factor Q is sufficiently large. Setting $|\min\mathcal{F}(\Omega\tau)| = 0.28$, and $\mathcal{R} = 0.16\text{-}0.32$, we obtain that Q should be fairly large: $Q > 25\text{-}50$. The latter requires $\nu \lesssim (1\text{-}2) \times 10^{11}\,\mathrm{s}^{-1}$. As a result, the self-excitation of the plasma oscillations in the G-TUNNETTs under consideration is possible only in sufficiently perfect graphene layers.

4. Conclusions

We demonstrated that the G-TUNNETT under consideration can exhibit the negative terminal dynamic conductivity in the THz range of frequencies due to the tunneling and transit-time effects in its i-section. Owing to this, G-TUNNETTs can be used in THz oscillators with a complementary resonant cavity. The generation of THz radiation is also possible due to the self-excitation of the plasma oscillations in the device p- and n-sections.

Acknowledgments

The authors are grateful to Professors T. Otsuji and M. Asada for stimulating discussions. The work was supported by the Japan Science and Technology Agency, CREST and the Japan Society for Promotion of Science, Japan, as well by the Airforce Office of Scientific Research, USA.

References

[1] C. Berger, Z. Song, T. Li, X. Li, A.Y. Ogbazhi, R. Feng, Z. Dai, A.N. Marchenkov, E.H. Conrad, P.N. First, W.A. de Heer, J. Phys. Chem. 108 (2004) 19912.
[2] S.V. Morozov, K.S. Novoselov, M.I. Katsnelson, F. Schedin, D.C. Elias, J.A. Jaszczak, A.K. Geim, Phys. Rev. Lett. 100 (2008) 016602.
[3] Xu Du, I. Skachko, A. Barker, E.Y. Andrei, Nat. Nanotechnol. 3 (2008) 491.
[4] V. Ryzhii, M. Ryzhii, V. Mitin, M.S. Shur, Appl. Phys. Express 2 (2009) 034503.
[5] V.V. Cheianov, V.I. Fal'ko, Phys. Rev. B 74 (2006) 041403 (R).
[6] V. Ryzhii, M. Ryzhii, T. Otsuji, Phys. Stat. Sol. (a) 205 (2008) 1527.
[7] L.M. Zhang, M.M. Fogler, Phys. Rev. Lett. 100 (2008) 116804.
[8] V. Ryzhii, A. Satou, T. Otsuji, J. Appl. Phys. 101 (2007) 024509.
[9] M. Dyakonov, M. Shur, IEEE Trans. Electron. Devices 43 (1996) 1640.
[10] V. Ryzhii, A. Satou, M. Shur, Phys. Stat. Sol. (a) 202 (2005) R113.